

Modeling Temporal Evolution of *Junco* Marshes Radar Signatures

Francisco Grings, Paolo Ferrazzoli, *Member, IEEE*, Haydee Karszenbaum, Javier Tiffenberg, Patricia Kandus, Leila Guerriero, and Julio C. Jacobo-Berrles

Abstract—In this work, multitemporal synthetic aperture radar (SAR) data in conjunction with an electromagnetic (EM) model and a vegetation growth model were used to monitor and explain burn-regrowth events of *junco* vegetation in a wetland environment. The data used were from Radarsat-1, ENVISAT Advanced Synthetic Aperture Radar (ASAR), and European Remote Sensing 2 (ERS-2) temporal series. The EM model is based on radiative transfer theory and describes *junco* vegetation as a set of vertical dielectric cylinders on a flat flooded surface. It was used, together with the vegetation growth model, to predict the temporal evolution of the radar response during a burn-regrowth event. This simulation was compared with the ERS-2 vertical (VV) data. It was observed a “bell-shaped” temporal trend that was confirmed by the simulated data with a mean error of 2.5 dB. Additionally, in view of current and future ENVISAT ASAR Alternating Polarization Mode Precision data, the horizontal (HH) SAR temporal response was also simulated giving as a result strong differences between simulated HH and VV temporal trends. These differences are in good agreement with the ones observed between Radarsat-1 HH and ERS-2 VV SAR data acquired at close dates and also with the same differences observed between HH and VV ENVISAT ASAR data. Electromagnetic modeling results provide a sound theoretical interpretation of these observations.

Index Terms—Electromagnetic (EM) models, radar, wetlands.

I. INTRODUCTION

WETLANDS are areas where the frequent and prolonged presence of water at or near the soil surface drives the natural system. An increasing use of remote sensing data to map and monitor wetland marshes, due to their importance and their deterioration and loss rate, is taking place. Through monitoring of wetland regions, an improved understanding of the water balance and stability of regional watershed systems can be obtained.

The utility of satellite radar data for understanding vegetation structure and hydrological conditions in wetlands has been

Manuscript received August 10, 2004; revised May 24, 2005. This work was supported in part by the Argentine institutions Consejo Nacional de Investigaciones Científicas y Técnicas (CONICET) and the University of Buenos Aires FCEyN and in part by the Argentine-Italy, Secretaria de Ciencia y Tecnología (SeCyT), Ministerio Affari Esteri (MAE) cooperation project.

F. Grings, H. Karszenbaum, and J. Tiffenberg are with the Instituto de Astronomía y Física del Espacio, Ciudad Universitaria, 1428 Buenos Aires, Argentina (e-mail: verderis@iafe.uba.ar).

P. Ferrazzoli and L. Guerriero are with the Tor Vergata University, Ingegneria—DISP, 00133 Roma, Italy.

P. Kandus is with the Universidad de Buenos Aires, FCEyN, Departamento de Biología, Laboratorio de Ecología Regional, Ciudad Universitaria, 1428 Buenos Aires, Argentina.

J. C. Jacobo-Berrles is with the Universidad de Buenos Aires, FCEyN, Departamento de Computación, Ciudad Universitaria, 1428 Buenos Aires, Argentina.

Digital Object Identifier 10.1109/TGRS.2005.855067

demonstrated extensively over the last decade. It is well documented through models and observations that when standing water is present beneath the vegetation canopies, the radar response changes depending on the dominant vegetation type, its density, and height. In wetlands dominated by herbaceous vegetation, increased flooding was detected by either an increase or a decrease in backscatter magnitude. Increases in backscatter result from an increase in double-bounce interactions between the vegetation and water surface, whereas decreases result from an increase in forward scattering off the open water (vegetation covered by water) [1]–[3], and/or canopy attenuation. All this depends on radar frequency and polarization and on canopy orientation, height, and density. Radar response is also strongly modified by changes in herbaceous vegetation structure (density and height) due to frequent burnings [4], [5]. Conversely, radar signals often increase in forested wetlands when standing water is present because of the strong differences in the trunk-ground contribution between nonflooded and flooded forest [6]–[10].

Two European Space Agency (ESA) projects, one providing European Remote Sensing 2 (ERS-2) synthetic aperture radar (SAR) data and the other ENVISAT Advanced Synthetic Aperture Radar (ASAR) Alternating Polarization Mode Precision (APP) data, address the Paraná River Delta, a fresh water wetland located very near Buenos Aires city. In addition, a program (Globesar II) supported by the Canada Centre for Remote Sensing made RADARSAT-1 data over the same area available [11]. Two main types of strong events affect this area, marsh burnings and unusual flooding events. In particular, the ERS-2 dataset was acquired during a dry period when frequent burnings followed by strong rains took place.

The main objective of this paper is to understand and explain through model simulations the observed temporal behavior of the SAR vertical (VV) response. In view of current and future acquisitions of ENVISAT ASAR APP data, the SAR horizontal (HH) response was also simulated. This paper also addresses the issue of the strong differences observed between VV and HH polarization (in both acquired and simulated values). This is done by combining radar observations, electromagnetic (EM) models, field work (vegetation characteristics), and environmental data (hydrologic and meteorological data).

Section II describes the characteristics of the area and the experimental data used in this study. Section III gives information about the model adopted to simulate the experimental results. The next sections address two subjects, ERS-2 radar observations of the temporal evolution of *junco* marshes growth from a burned condition to a mature status and its interpretation (Section IV), and a discussion of the polarization properties of *junco* marshes as seen in the VV and HH simulated values and ob-

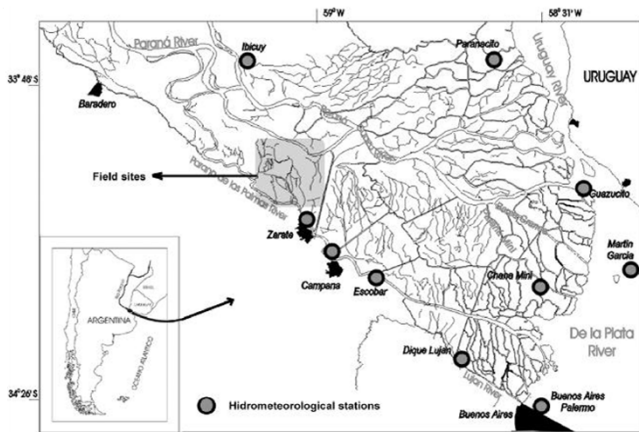


Fig. 1. Study site.

served by ERS-2, RADARSAT-1, and ENVISAT ASAR data (Section V). The final section summarizes the results obtained and the main conclusions.

II. STUDY SITE AND EXPERIMENTAL DATA

The Delta of the Paraná River is one of the most important wetland systems of Argentina and South America. It extends along 300 km from 32° 5' S, Diamante city in Entre Rios Province to 34° 29' S near Buenos Aires City through the terminal portion of the De la Plata River basin covering 17 000 km². It is constituted by a heterogeneous mosaic of landscape patterns which are subject to a complex flooding regime that results mainly from the influence of Paraná, Uruguay, and De la Plata rivers. In particular, the Paraná River is the only one of the large rivers of Argentina that flows from the humid tropics to temperate regions. This determines the coexistence of species of tropical lineage and temperate latitudes. Also, the area has been strongly modified by anthropogenic effects such as large forest plantations of *Salix spp.* and *Populus spp.*, tourists sites, and infrastructure developments.

The landscape patterns of this region are subordinated to a flooding regime characterized by different sources of water with a different behavior, i.e., local precipitation, and large rivers whose specific flooding patterns affect particular areas. Sometimes these sources add together provoking large flooding events. The greatest influence comes from Parana's River which shows a main flood peak in late summer and a second peak in winter. Nevertheless, the flooding patterns of Gualeguay River in the middle and lower part and of the Uruguay River in the terminal part also affect this area. The final portion is also influenced by the De La Plata River with its daily wind and lunar tides. This complex system not only shows seasonal variations but also annual and interannual fluctuations.

Fig. 1 shows the terminal part of this Delta which is the area addressed by the radar projects in progress. Table I summarizes the main land covers present in this area, their characteristics and soil condition. Table II summarizes the SAR data used and their characteristics.

It must be stressed the fact that the temporal ERS-2 sequence covers two different environmental conditions, a very dry 1999 year and a wet 2000 year. Continuous burnings of the *junco*

TABLE I
STUDY SITE LAND COVER TYPES AND CHARACTERIZATION

Land Cover Type	Junco marshes	Cortadera marshes	Poplar Forest (dike)	Willow Forest (dike)	Willow Forest (channels & drains)
Characteristics					
Dominant species	<i>Schoenoplectus californicus</i>	<i>Scirpus giganteus</i>	<i>Populus spp.</i>	<i>Salix spp.</i>	<i>Salix spp.</i>
Plant coverage (%)	< 80	100	< 100	< 100	< 100
Plant Height (m)	2.0 - 2.5	1.5 - 2.0	> 10	> 10	> 10
Plant Phenology	Perennial	Perennial	Deciduous	Deciduous	Deciduous
Soil Condition	Permanently flooded (normal flood condition)	Saturated	Dry	Dry	Alternatively dry or saturated

TABLE II

SAR SYSTEMS CHARACTERISTICS, ACQUISITION DATES, AND SEASONS. JULIAN DAYS FROM JANUARY 1, 1999 ARE INDICATED IN PARENTHESIS. ERS-2 DATA SEQUENCE COVERS TWO DIFFERENT ENVIRONMENTAL CONDITIONS, A VERY DRY 1999 YEAR WHEN FIRE EVENTS TOOK PLACE AND A WET 2000 YEAR WITH HEAVY RAINS

System	ERS 2 SAR	RADARSAT S1	ENVISAT S1
Characteristics			
Dates	June 5/1999 (156) - Winter July 10/1999 (191) - Winter Aug 14/1999 (226) - Winter September 18/1999 (261) - Winter October 23/1999 (295) - Spring February 5/2000 (399) - Summer March 11/2000 (436) - Summer April 15/2000 (471) - Autumn May 20/2000 (505) - Autumn June 24/2000 (541) - Winter July 29/2000 (576) - Winter September 2/2000 (611) - Winter December 14/2000 (711) - Spring	Dec 11/2000 - Spring	Nov 20/2003 - Spring
Band	C	C	C
Polarization	VV	HH	HH, VV
Incidence angle	23 °	23.5 °	19 °

marshes took place during the 1999–2000 spring-summer months (from October–March). These are the overall environmental conditions behind the radar observations analyzed and modeled.

The input parameters to the model were obtained from field campaigns carried out by P. Kandus and her team [12]. Satellite optical data, provided by the Argentine National Space Activities Commission (CONAE), taken at dates close to the SAR data acquisition, were used to help and support interpretation. Auxiliary data such as river levels and precipitation were provided by the Argentine National Water Institute (INA) and the Argentine Navy Hydrographic Service (SHN).

III. MODEL DESCRIPTION

Junco marshes have been modeled as a set of vertical cylinders (shoots) defined by a radius, height, density and gravimetric moisture, on a normal flooded surface (Fig. 2).

In this work, we have used the model developed at “Tor Vergata” University [13]. In its general version, it is a model based on the radiative transfer theory, which subdivides the vegetation into homogeneous layers filled with discrete elements. After the scattering and extinction cross sections of single elements have been computed, the single contributions are joined together, and finally, the overall vegetation effects are combined with soil effects. Details about the general procedure are given in [13].

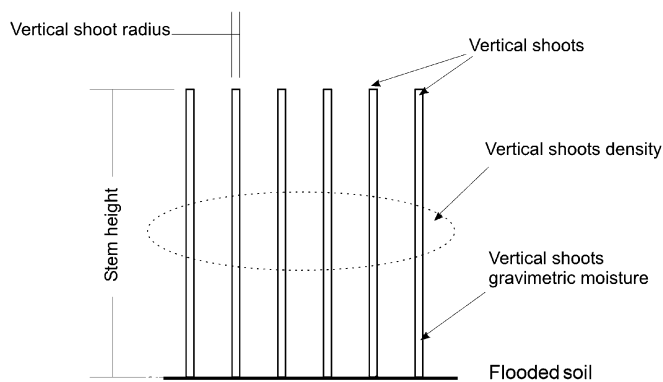


Fig. 2. Elements characterizing the junco marshes model.

For the case of *junco* marshes, a simplified version has been adopted, since only the following two main scattering sources have been considered:

- top layer, containing vertical cylinders representing shoots;
- lower half-space, representing the soil.

Each layer is characterized by a set of physical and geometrical parameters, also defined in Fig. 2. For vertical cylinders, the dielectric constant has been computed through the semiempirical formula, given in [14], which needs the moisture content as input. Then, the infinite length approximation [13], which approximates the field inside a finite cylinder with that of an infinite one, has been used for the calculation of the extinction, backscattering and specular scattering cross-sections. This approximation is valid when the half-length of the cylinder is much higher than the radius, a condition satisfied by the *junco* marshes dimensions. When the *junco* marshes reach the mature state, they become dense, partially dry, and lose vertical orientation. For these conditions, they have been modeled as a volume of randomly oriented cylinders. The basic methodology of [13] may be applied also in this case.

The dielectric constant of soil is generally related to its moisture contents. Since we are mostly concerned with normally flooded soils, it has been set equal to pure water dielectric constant. The EM properties of the soil are described by its bistatic scattering coefficient. According to the analysis developed in [16], this coefficient is given by the superposition of a specular coherent contribution and a diffuse incoherent contribution. The coherent contribution, which is proportional to the specular reflectivity given in [16] and [17], is dominant in our case, since a very flat surface (i.e., with rms height equal to 0.1 cm), has been assumed to represent the normally flooded soil. Once the soil and the shoots were characterized, their contributions were combined by using the procedure described in [13]. The procedure gives the total backscattering coefficient as output. Also single contributions may be evaluated: soil direct backscattering, shoot direct backscattering, soil/shoot double-bounce interaction.

IV. MULTITEMPORAL EVOLUTION

Qualitative site-specific observations of *junco* marshes show that following a relatively intense burn, a burnt site progresses from grass stubble to short mostly vertical green shoots. During the regrowth, the height of the young green shoots increases rapidly, while density of the canopy increases at a slower rate, taking about a few months to reach the average density, although

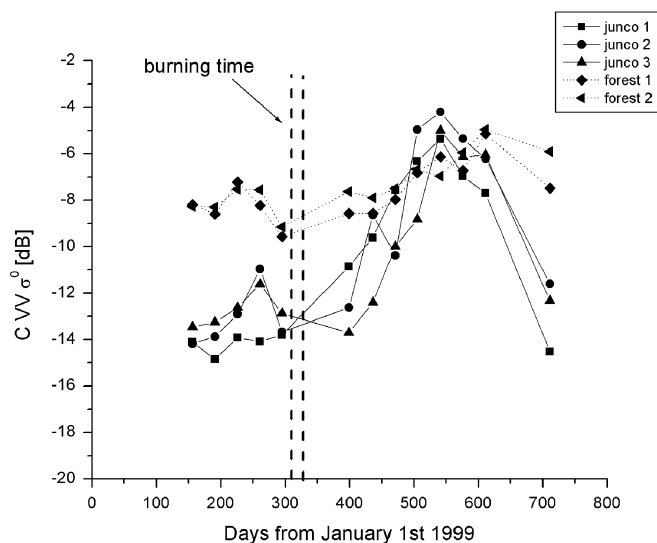


Fig. 3. Temporal trends of backscattering coefficients collected by ERS-2 over junco marshes and forests. Dashed lines indicate the burning period.

complete maturity may be reached at a later stage. In this later stage, green and dry shoots are present. A similar behavior was reported in the recovery of juncos *roemerianus* marsh burns [4], [5]. Following this description, *junco* marshes may be characterized as indicated below:

Vegetation status:

- young juncos (green shoots, medium height, low density);
- mature juncos (mixing of green and dry shoots, maximum height, maximum density);
- burned juncos (burned shoots, very low values of density, height and moisture);

Soil status:

- soil not covered by water;
- soil covered by a water layer of few centimeters (normal flood condition);
- soil covered by a water layer of about a meter height (after strong flooding).

Soil states may depend on the level of Paraná River, precipitation and intense meteorological phenomena (e.g., El Niño occurrence). During the time period considered in this publication, only the second soil condition was observed.

Our ERS-2 observations on this area indicate that the *junco* marshes show the characteristic behavior of Fig. 3, with large variations (from -14 to -5 dB) of total σ^0 . This is not observed in other areas, such as forests, whose backscattering coefficients are shown for reference. In general, these variations may be related to the level of flooding and the *junco* vegetation structural condition (burned, young, mature) [12]. However, in this specific area, the soil is covered by a water layer of few centimeters most of the time. Therefore, we can state that the variations of σ^0 were due to changes in *junco* structure, related to plant growth or plant destruction by burning.

We have investigated this effect using the model. To this aim, we have used some assumptions about the *junco* growing process, which are important to give correct inputs to the model. It has been verified that shoot radius and shoot moisture show limited variations during the *junco* growth cycle. In fact, the model was run by assigning to these variables constant values,

TABLE III
INPUT VARIABLES FOR THE MODEL

Parameter	Value	Comments
Frequency	5.0 GHz	C-band
r.m.s height	0.1 cm	Normal flooded soil
Correlation length	10.0 cm	Normal flooded soil
Gravimetric soil moisture	1.0 g/g	Pure water
Vertical shoot radius	0.5 cm.	From [12]
Vertical shoot gravimetric moisture	0.7 g/g	From [12]
Vertical shoot height	Young juncos = 10 – 100 cm Mature juncos = 150 – 200 cm	From [12]
Vertical shoot plant density	Young juncos = 10 – 30 m ² Mature juncos = 75 – 100 m ²	From [12]

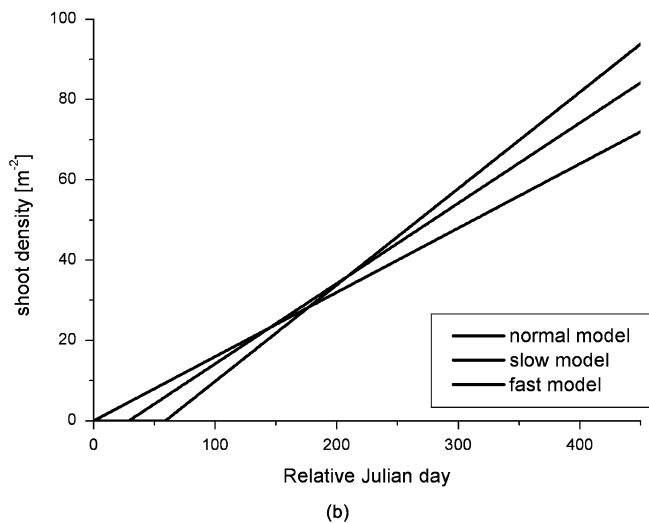
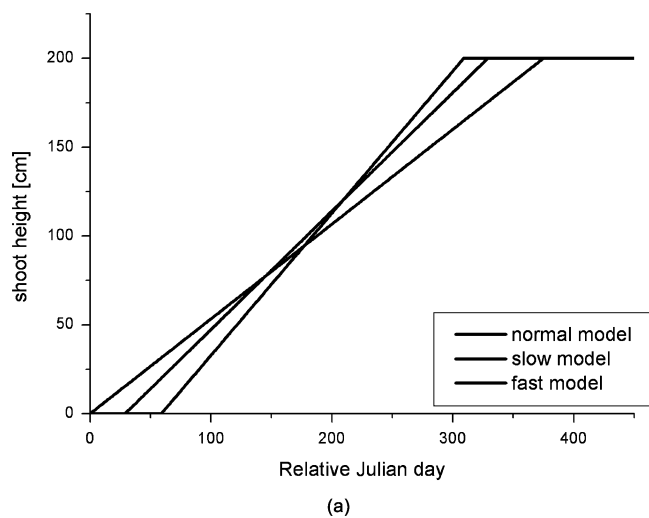


Fig. 4. Simplified empirical models for the variations of (a) height and (b) density of juncos during plant regrowth. Growth models were expressed as slow model ($d = 0.15t, h = 0.55t$), normal model ($d = 0.2t - 30, h = 0.66 - 30$), and fast model ($d = 0.25t - 60, h = 1.2t - 60$), where d is *junco* plant density, h is *junco* height, and t is time in Julian days.

which are given in Table III. Therefore, the most important variables, influencing temporal variations of backscattering coefficient, are the shoot height and the shoot density. It has been observed that recently burned juncos undergo a rapid height increase, during the first few months, and after that there is an increase in density. Therefore, although specific temporal characteristics may be different among the single areas, the basic scheme indicated in Fig. 4(a) and (b) are generally valid. We

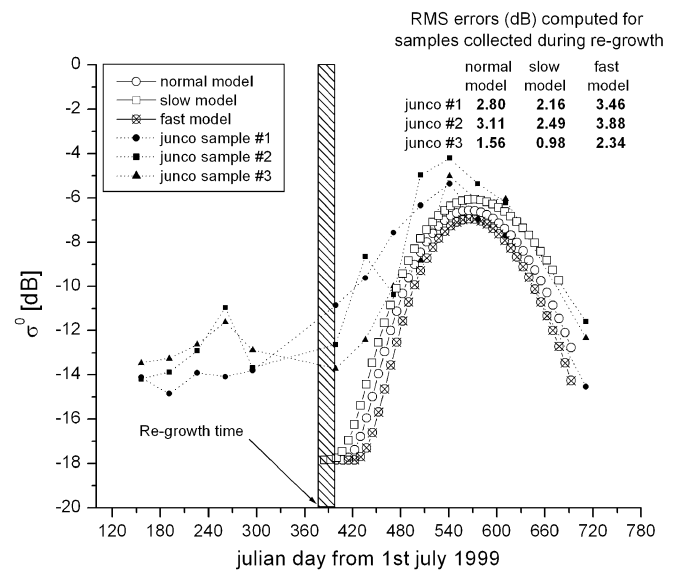


Fig. 5. Simulated backscattering coefficients (C-band, VV, 23° incidence angle) of the three proposed regrowth schemes. Three temporal trends of σ^0 collected by ERS-2 over junco marshes are shown. The quadratic error in decibels between every model simulation and every junco sample is also shown. Shoot radius = 0.5 cm; moisture = 0.7 g/g.t

have considered three different biological regrowth schemes, related to three linear model specifications, also described in Fig. 4. We know from field work that the most probable growing scheme is the one labeled “normal model.” Anyway, it is possible to think of junco areas with different environmental conditions (water access, different concentration of soil nutrients) in which the growing procedure is faster or slower. Furthermore, the exact burning time of every junco area is not exactly known, so it is also possible that there were different burning times for different areas. This is why we simulate the response of different growing schemes, by assuming the days of maximum radar response to be the same for all cases.

By adopting these assumptions, we have simulated the temporal evolution of *junco* backscattering coefficient by considering the whole range of variations for height and density and by assuming the radius and the moisture to have the fixed values indicated in Table III. Results are shown in Fig. 5, where σ^0 is plotted as a function of time for the three regrowth schemes, and ERS-2 SAR signatures are again shown for comparison.

After burning, low σ^0 values (about -14 dB) are observed. An increase in height, with low density values, produces an increase of σ^0 , up to a maximum of about -5 dB (for a height of 125 cm and a density of 20 m⁻²). After that, an increase of density and a further increase of height produce a decrease of σ^0 . Therefore, there is a general agreement between the experimental trends of Fig. 3 and the simulation scheme of Fig. 5. Also RMS errors are shown.

By looking at the single scattering components, we have observed that the main interaction mechanism is the junco–soil double-bounce interaction. This is due to the junco vertical orientation, and to the fact that we are considering an almost flat flooded soil.

Interpretation of results is given below.

- 1) Just after burning (as in October–November, 1999), the surface consists of soil covered by water and few residual

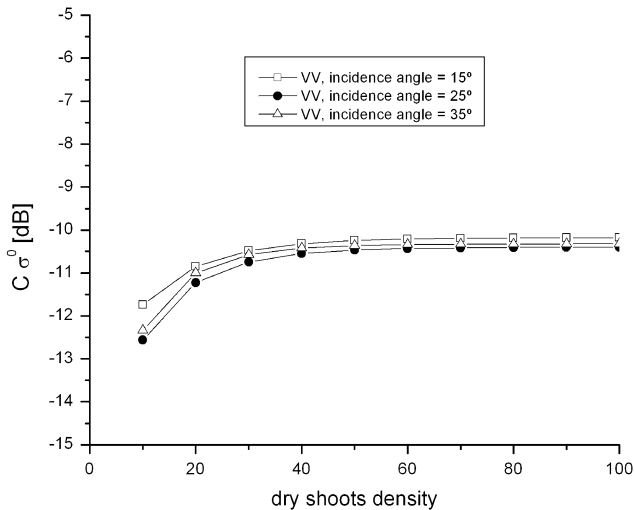


Fig. 6. Total backscattering coefficient for VV polarization as a function of shoot density for drying shoots. Height = 2 m, radius = 0.5 cm, moisture = 0.4 g/g. Shoots are subdivided into randomly oriented sections.

burned *junco* shoots. These shoots are dry, due to burning, and loose the vertical orientation which is required to produce a high double-bounce scattering. The overall effect is a low backscattering coefficient (about -14 dB in Fig. 3).

- 2) During the growing phase after burning (February-May, 2000) there is a rapid increase of height, while the increase in density is slow. The σ^0 increase observed during this phase is reproduced by our simulations, and may be explained with an increase in soil-shoot double-bounce backscattering, while attenuation does not yet increase so much.
- 3) The effect mentioned in the previous point lasts until a maximum σ^0 is achieved (June 2000, approximately -5 dB), corresponding to a combination of height and density, which enhances this effect.
- 4) In the following phase (July–December, 2000), the shoot density increases, producing an increase in the attenuation and, hence, a decrease in the backscattering coefficient.
- 5) According to the model, a further increase in the density would lead to very low backscattering values (about -20 dB). However, these very low values are not observed in experimental data. This last effect may be explained if we consider that shoots are drying at the end of their cycle. Therefore, their moisture decreases up to about 0.4 g/g, which is lower than the value of 0.7 g/g adopted in the simulation of Fig. 5. Moreover, the long shoots loose their vertical structure and tend to be subdivided into short sections. By simulating this structure, the results shown in Fig. 6 have been obtained. In this case, the backscattering coefficient is slightly influenced by incidence angle and density. These properties may be interpreted by considering that the attenuation is still high, but the random orientation of shoot sections produces an appreciable direct scattering from *junco* marshes. The backscattering coefficient tends to values lower than -10 dB, but appreciably higher than in the case of simulations using only dense vertical shoots. In addition, the simulated values including the dry shoots layer are closer to the end of cycle of the experimental data shown in Fig. 3 (from -12 to -14 dB).

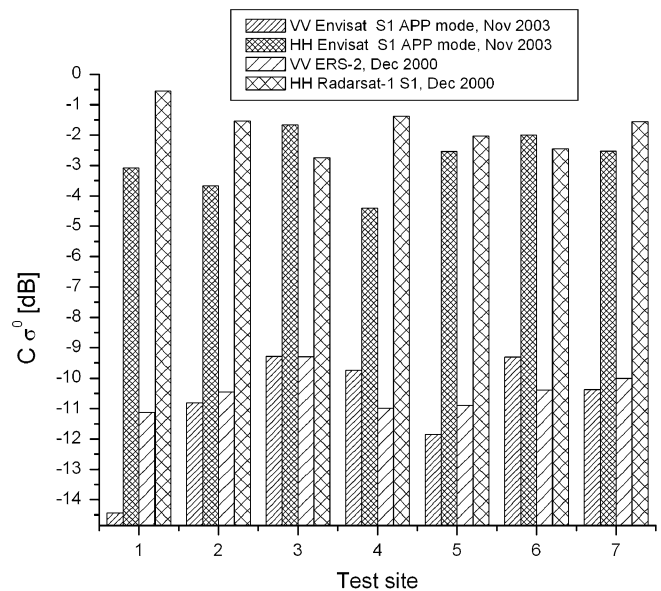


Fig. 7. HH and VV σ^0 of *junco* marshes collected by RADARSAT-1 (S1) and ERS-2, and HH and VV σ^0 of *junco* marshes collected by ENVISAT alternating polarization mode (S1).

V. EFFECT OF POLARIZATION IN MODELED MULTITEMPORAL EVOLUTION

In a previous study, where ERS-2 and RADARSAT-S1 images were acquired over the Delta del Paraná region, a remarkable difference of the order of 10 dB was observed between HH and VV radar responses for *junco* marshes [11]. The passages of the two satellites were not simultaneous, but the delay was three days. Furthermore, during 2003, ENVISAT S1 (19° mean incidence angle) data have been acquired over the same areas covered by *junco* marshes, and a similar mean difference was observed. These observations are summarized in Fig. 7.

Although the three instruments are different, data obtained by ENVISAT are similar to the ones obtained in [11], which confirms that this difference between HH and VV backscattering coefficients is characteristic of normally flooded *junco* marshes.

For the time being, we do not have a RADARSAT-1 or ENVISAT ASAR dual-polarization temporal series similar to the ERS-2 one of Fig. 3. However, we have simulated the HH radar response in the regrowth process using the model. The results are shown in Fig. 8. At the first growing stages, HH is smaller than VV because short and sparse cylinders produce a lower scattering at H polarization. Nevertheless, as soon as the *junco*s grow, HH begins to dominate over VV. This is due to three different processes: 1) cylinder bistatic specular scattering is higher in the case of H incident polarization than in V one (C-band $\sigma_{sh} > \text{C-band } \sigma_{sv}$), 2) soil bistatic specular scattering (Fresnel coefficient) is higher at H polarization than at V one ($C F_H > C F_V$); and 3) shoot attenuation (extinction coefficient), is higher at V than at H one ($C \sigma_{ev} > C \sigma_{eh}$). Fig. 9 illustrates an overall scheme of the *junco* marshes model, showing the dominant interaction mechanism and the relationships between the parameters that determine the polarization differences in double-bounce-type interactions.

To investigate the validity of these assumptions about the HH VV differences, the radiative transfer model was used for a parametric investigation. Fig. 10 shows a simulation of σ^0 HH

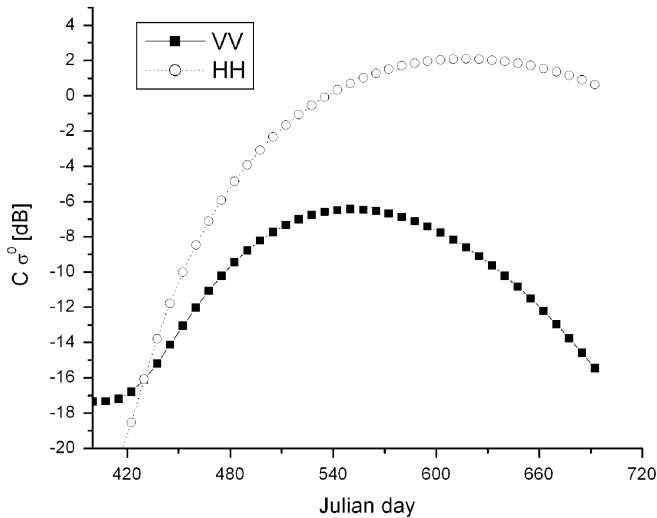


Fig. 8. Simulated backscattering coefficients (C-band, 23° incidence angle) for both polarizations of the normal regrowth scheme.

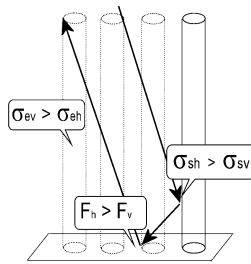


Fig. 9. Overall scheme of the *junco* model. The *junco*–soil double-bounce mechanism and the key process variables are shown. They are: 1) the specular bistatic scattering coefficient over the *junco* surface (σ_s); 2) the Fresnel coefficient for a rough surface (F), and 3) the extinction coefficient of the vertical *juncos* (σ_e).

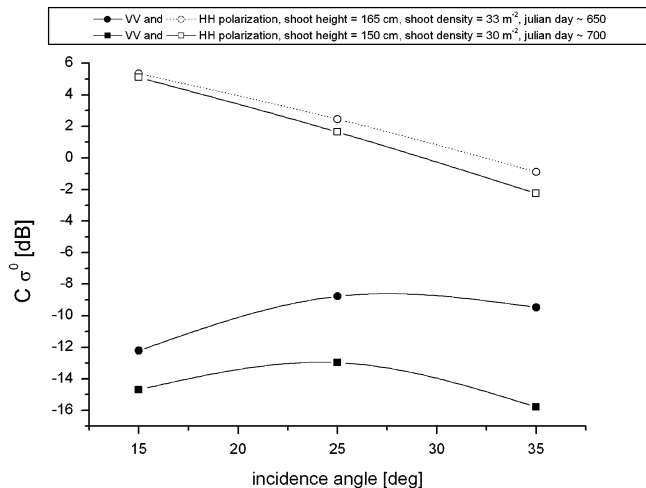


Fig. 10. Total backscattering as a function of incidence angle for both polarizations and two different height-density conditions.

and VV as a function of incidence angle for both polarizations and two different height-density conditions. The difference observed is related, as we previously mentioned, to the *junco*–soil double-bounce interaction. These simulations represent average situations of mature *juncos*, so the σ^0 simulated values can be compared with experimental ones of Fig. 7.

Anyway, some simulated values are slightly higher than the ones observed. This can be explained if we take into account the fact that the assumption of perfectly vertical, straight, constant section stems used in the theoretical model is only an ideal case. In reality, *junco* shoots are not perfectly vertical, are partially bent, and have a slightly varying section as we go from the base to the top.

VI. SUMMARY AND CONCLUSION

The Delta of the Paraná River was observed by ERS-2 SAR during years 1999 and 2000, which were characterized by a dry period followed by a wet period. From October 1999 to the end of the summer (March), some *junco* marshes suffered burning events, followed by regrowth. ERS-2 signatures proved to be able to monitor these events, showing an increase of σ^0 soon after burning, followed by a decrease observed during the phase of full development and senescence. An EM model, describing *junco* shoots as dielectric cylinders over a flooded surface, reproduces this trend, and interprets it as the consequence of a complex balance between cylinder scattering and cylinder attenuation. The simulations cover two different vegetation conditions. The first one refers to green vertical cylinders with increasing densities and heights. The second one addresses the complete mature *juncos* for which a layer of dry *juncos* with random orientation was considered. This two-step simulation provides a good explanation of observations.

The availability of radar data of different polarizations reveals strong differences in the HH VV radar response. One of the datasets, acquired in December 2000 consists of an ERS-2 and a RADARSAT-1 scene. The other set was directly collected by ENVISAT ASAR. The two datasets agree in showing a difference of 6 to 9 dB between HH and VV σ^0 's.

Although at present time extended dual-polarized multitemporal signatures are not available to us, the simulation results described in this work indicate that a dual-polarization system may be more powerful than a single polarized one for detecting and monitoring *junco* areas, and for retrieval applications. We show that a radiative transfer model can successfully simulate the VV radar response of a *junco* regrowth process. Furthermore, we also show that the sensitivity to *junco* plant density is higher at VV polarization than at HH (Fig. 10). This leads to a clear difference between HH and VV multitemporal regrowth trends (see Fig. 8) and, hence, to an improved monitoring potential associated to the availability of a dual-polarization system.

ACKNOWLEDGMENT

The authors thank J. M. Martinez who helped with the analysis of the ERS-2 temporal series at the beginning of the work with radar data, and graduate students P. Pralongo, G. Parmuchi, and G. Trilla for their contribution during field work campaigns. The authors specially thank the Canadian Centre for Remote Sensing GLOBESAR II program for providing RADARSAT-1 data, the European Space Agency for the continuous support through AO3 232 and AO 667 supported projects, the National Commission for Space Activities (CONAE) for the optical data, the National Water Institute (INA), and the National Hydrologic Service (SHN) for providing us river water levels and precipitation data.

REFERENCES

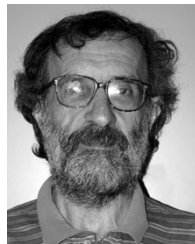
- [1] K. O. Pope, E. Rejmankova, F. F. Paris, and R. Woodruff, "Detecting seasonal flooding cycles in marshes of the Yucatan peninsula with SIR-C polarimetric radar imagery," *Remote Sens. Environ.*, vol. 59, pp. 157–166, 1997.
- [2] E. S. Kasischke, K. B. Smith, L. L. Bourgeau-Chavez, E. A. Romanowicz, S. Brunzell, and C. J. Richardson, "Effects of the seasonal hydrologic patterns in South Florida wetlands on radar backscatter measured on ERS-2 SAR image," *Remote Sens. Environ.*, vol. 88, pp. 423–441, 2003.
- [3] M. G. Parmuchi, H. Karszenbaum, and P. Kandus, "Mapping the Paraná River delta wetland using multitemporal RADARSAT/SAR data and a decision based classifier," *Can. J. Remote Sens.*, vol. 28, pp. 1202–1213, 2002.
- [4] E. W. Ramsey, III, S. K. Sapkota, F. G. Barnes, and G. A. Nelson, "Monitoring the recovery of juncos roemerianus marsh burns with the normalized difference vegetation index and Landsat Thematic Mapper data," *Wetlands Ecol. Manage.*, vol. 10, pp. 85–96, 2002.
- [5] E. W. Ramsey, III, G. A. Nelson, S. K. Sapkota, S. C. Laine, J. Verdi, and S. Krasznay, "Using multiple polarization L-Band radar to monitor marsh burn recovery," *IEEE Trans. Geosci. Remote Sens.*, vol. 37, no. 1, pp. 635–639, Jan. 1999.
- [6] J. A. Richards, P. W. Woodgate, and A. K. Skidmore, "An explanation of enhance of radar backscattering from flooded forests," *Int. J. Remote Sens.*, vol. 8, pp. 1093–1100, 1987.
- [7] L. L. Hess, G. M. Melack, and D. S. Simonett, "Radar detection of flooding beneath the forest canopy, a review," *Int. J. Remote Sens.*, vol. 11, pp. 1313–1325, 1990.
- [8] L. L. Hess, J. M. Melack, S. Filoso, and Y. Wang, "Delineation of inundated area and vegetation along the amazon floodplain with the SIR-C synthetic aperture radar," *IEEE Trans. Geosci. Remote Sens.*, vol. 33, no. 4, pp. 896–902, Jul. 1995.
- [9] P. A. Townsend, "Mapping seasonal flooding in forested wetlands using multitemporal radarsat SAR," *Photogramm. Eng. Remote Sens.*, vol. 67, pp. 857–864, 2001.
- [10] —, "Estimating forest structure in wetlands using multitemporal SAR," *Remote Sens. Environ.*, vol. 79, pp. 288–304, 2002.
- [11] H. Karszenbaum, P. Kandus, J. M. Martinez, T. L. Toan, J. Tiffenberg, and G. Parmuchi, "ERS-2, RADARSAT SAR backscattering characteristics of the Paraná River delta wetlands, Argentina," in *ERS-Envisat Symp.*, 2000, ESA-SP-461.
- [12] P. Kandus and P. Pratalongo, private communication, 2002.
- [13] M. Bracaglia, P. Ferrazzoli, and L. Guerriero, "A fully polarimetric multiple scattering model for crops," *Remote Sens. Environ.*, vol. 54, pp. 170–179, 1995.
- [14] M. A. El-Rayes and F. T. Ulaby, "Microwave dielectric spectrum of vegetation—Part I: Experimental observations," *IEEE Trans. Geosci. Remote Sens.*, vol. GE-25, pp. 541–549, 1987.
- [15] M. A. Karam and A. K. Fung, "Electromagnetic scattering from a layer of finite length, randomly oriented, dielectric, circular cylinders over a rough interface with application to vegetation," *Int. J. Remote Sens.*, vol. 9, pp. 1109–1134, 1988.
- [16] R. Schiffer, "Reflectivity of a slightly rough surface," *Appl. Opt.*, vol. 26, pp. 704–712, 1987.
- [17] P. Beckmann and A. Spizzichino, *The Scattering of Electromagnetic Waves From Rough Surfaces*. New York: Pergamon, 1963.



Francisco Grings graduated in medical physics from the Universidad de San Martín, San Martín, Argentina, in 2003. He is currently pursuing the Ph.D. degree at the Instituto de Astronomía y Física del Espacio (IAFE), Buenos Aires, studying "the retrieval of biophysical variables from coastal wetlands using SAR systems and EM modeling."

In 2002, he joined the Remote Sensing Group of the IAFE. In 2004, as a part of the IAFE Remote Sensing Group cooperation with DISP—Tor Vergata, he was in Rome with Paolo Ferrazzoli for one month,

adapting marsh radiative transfer models to simulate ASAR radar response in marshes. He is currently involved in a collaboration project related to the Argentine SAOCOM SAR mission.



Paolo Ferrazzoli (M'95) graduated from the University of Rome "La Sapienza," Rome, Italy, in 1972.

In 1974, he joined Telespazio S.p.A., Rome, Italy, where he was mainly active in the fields of antennas, slant-path propagation, and advanced satellite telecommunication systems. In 1984, he joined the University of Rome, "Tor Vergata," Rome, Italy, where he is presently working, teaching microwaves and propagation. His current research is focused on microwave remote sensing of vegetated terrains, with particular emphasis on electromagnetic modeling. He has been involved in international experimental remote sensing campaigns such as AGRISAR, AGRISCATT, MAESTRO-1, MAC-Europe, and SIR-C/X-SAR. He has participated with the coordinating team of the ERA-ORA Project, funded by the EEC, establishing an assemblage among several European researchers working in radar applications. He has been a member of the Science Advisory Group of the European Space Agency's SMOS Project.



Haydee Karszenbaum graduated in physics from the University of Tennessee, Knoxville.

In 1979, she joined the Consejo Nacional de Investigaciones Científicas y Técnicas (CONICET), Buenos Aires, Argentina. In 1982, she began doing Remote Sensing work at University of Delaware, Newark, in coastal applications. Since then she has participated in several projects related to the study of Argentine coastal areas using optical and thermal remote sensing data. From 1997 on, she has been working in radar remote sensing, mainly in wetland applications. She was the Principal Investigator (PI) of a Radarsat 1 GlobSAR 2 project and of an ESA ERS-2 AO3 232 project. She is currently PI of the ENVISAT ASAR AO 667 project and of a national project on radar remote sensing financed by the Secretaría de Ciencia y Tecnología, Argentina. Since 1994, she has been collaborating with the National Commission on Space Activities (CONAE). She is also currently involved in a collaboration project related to the Argentine SAOCOM SAR mission.



Javier Tiffenberg is currently studying physics at the University of Buenos Aires (UBA), Buenos Aires, Argentina.

In 2000, he joined the Remote Sensing Group of the Astronomy and Space Physics Institute (IAFE), Buenos Aires, where he is currently working in the retrieval of biophysical variables from and EM modeling. He is currently involved in a collaboration project related to the Argentine SAOCOM SAR mission.



Patricia Kandus graduated from the University of Buenos Aires, Buenos Aires, Argentina, in 1985.

At that time, she joined the Laboratory of Regional Ecology at the Faculty of Sciences and started working in wetland ecology. She focused her ecological studies in the Parana River Delta Region. At present, her research is focused on wetland vegetation structure and dynamics with particular emphasis on classification and monitoring using optical and microwave remote sensing.



Leila Guerriero received the laurea degree in physics from the University of Rome “La Sapienza,” Rome, Italy, and the Ph.D. degree in electromagnetism from the University of Rome “Tor Vergata,” in 1986 and 1991, respectively.

In 1988, she was involved in a cooperation between the Jet Propulsion Laboratory and the Italian National Research Council for investigations on geophysical applications of imaging spectrometry in infrared and visible remote sensing. In 1995, she participated in the ESA project concerning radiometric polarimetry

of the sea surface. In 1999 to 2001, she participated in the EEC concerted action ERA-ORA whose objective was to improve radar data analysis and utilization. More recently, she has been involved in the ESA SMOS project. Her activities at “Tor Vergata” are mainly concerned with modeling microwave backscattering and emissivity from agricultural and forested areas.



Julio C. Jacobo-Berrles received the Eng. degree in electronics and the Ph.D. degree in computer science from the University of Buenos Aires, Buenos Aires, Argentina, in 1983 and 2005, respectively.

His current research interests include microwave remote sensing, image processing, and computer vision. He is currently an Adjoint Professor at the Computer Science Department, Faculty of Exact and Natural Sciences, University of Buenos Aires and is currently involved in a collaboration project related to the Argentine SAOCOM SAR mission.